



# Real-time optimal spatiotemporal sensor placement for monitoring air pollutants

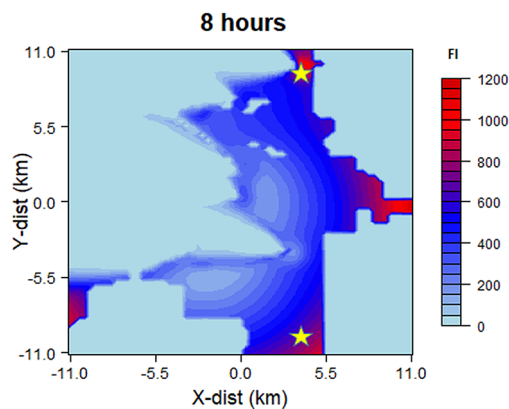
Rajib Mukherjee<sup>1,2</sup> · Urmila M. Diwekar<sup>1</sup> · Naresh Kumar<sup>3</sup>

Received: 15 January 2020 / Accepted: 30 September 2020 / Published online: 24 October 2020  
© Springer-Verlag GmbH Germany, part of Springer Nature 2020

## Abstract

Air pollution exposure assessment involves monitoring of pollutant species concentrations in the atmosphere along with their health impact assessment on the population. Often air pollutants are monitored via stationary monitoring stations. Due to the cost of sensors and land for the installation of the sensors within an urban area as well as maintenance of a monitoring network, sensors can only be installed at a limited number of locations. The sparse spatial coverage of immobile monitors can lead to errors in estimating the actual exposure of pollutants. One approach to address these limitations is dynamic sensing, a new monitoring technique that adjusts the locations of portable sensors in real time to measure the dynamic changes in air quality. The key challenge in dynamic sensing is to develop algorithms to identify the optimal sensor locations in real time in the face of inherent uncertainties in emissions estimates and the fate and transport of air pollutants. In this paper, we present an algorithmic framework to address the challenge of sensor placement in real time, given those uncertainties. Uncertainty in the system includes location and amount of pollutants as well as meteorology leading to a stochastic optimization problem. We use the novel better optimization of nonlinear uncertain systems (BONUS) algorithm to solve these problems. Fisher information (FI) is used as the objective of the optimization. We demonstrate the capability of our novel algorithm using a case study in Atlanta, Georgia. Our real-time sensor placement algorithm allows, for the first time, determination of the optimal location of sensors under the spatial–temporal variability of pollutants, which cannot be accomplished by a stationary monitoring station. We present the dynamic locations of sensors for observing concentrations of pollutants as well as for observing the impacts of these pollutants on populations.

## Graphic abstract



Optimal Sensor Placement for Atlanta, Georgia using Fisher information (FI) based on concentration of particulate matter (PM) at 8 a.m.

**Keywords** Spatiotemporal sensor placement · BONUS algorithm · Weather uncertainties · Stochastic optimization · Exposure assessment

Extended author information available on the last page of the article

## Introduction

The term “health risk” is defined by the qualitative and quantitative evaluation of health damage, disease, or death resulting from the actual or potential presence and/or exposure to specific pollutants. The main goal of risk analysis is to define the level of hazard posed to both individual human health and the health of the whole population in the selected area. Exposure assessment is an important step in health impact assessment, which depends upon the monitoring of pollutant species in the atmosphere. Exposure-based model for optimal sensor placement algorithms has been developed for water network systems by different researchers. Berry et al. (2005) considered water demand throughout the day with a fixed set of patterns without considering uncertainty and used a deterministic optimization method. Shastri and Diwekar (2006) have applied demand uncertainty and solved the problem using stochastic optimization. Both Berry et al. (2005) and Shastri and Diwekar (2006) have the objective of minimizing the fraction of the population exposed to contamination on the affected nodes. Mukherjee et al. (2017) considered demand as well as contamination location uncertainty for sensor placement for health impact reduction not only in the sensor node but also in subsequent downstream nodes.

Compared to the water network system, there are very few algorithms available for spatiotemporal air quality monitoring. In this work, we present a novel exposure-based model for optimal sensor placement in air pollution monitoring. Currently, air pollutant species are monitored via stationary monitoring stations with sparse coverage due to a limited number of sensors because of the high capital cost of installation, especially within an urban metropolitan area. Lack of coverage can lead to errors in the estimate of actual exposure to individuals. With the advancement of drone technologies, it is possible to measure the dynamic changes in air and water quality monitoring with unmanned aerial systems (UAS) (Tmuši'c et al. 2020). UAS have been extensively used for agriculture, vegetation, soil moisture, and river monitoring, as shown in Manfreda et al. (2018). Diwekar and Mukherjee (2017) have developed an algorithm for water quality monitoring with portable sensors that change positions in real time. Pattern recognition techniques have been used by Jácome et al. (2018) for optimal sensor placement in water quality monitoring. They have used cluster analysis to capture the temporal variation of pollutants. However, there are few works on the use of UAS for air quality monitoring. This type of dynamic sensing requires novel algorithms that decide sensor locations in real time in the face of inherent uncertainties in the fate and transport of the pollutants. Sun et al. (2019), in their paper, has developed

optimal sensor placement in the Gaussian spatial field for environmental monitoring using hourly air quality monitoring data from a particular year provided by Hong Kong Environment Protection Department (EPD). They did not track the source of pollutants or, in that sense, the fate and transport of pollutants. Efficient sensor placement for spatiotemporal sensor placement has been shown by Nguyen et al. (2018). The effectiveness of their proposed algorithm is demonstrated only in a small spatial environment like the scale of a university building. In this work, we have developed an algorithmic framework to solve the problem of sensor placement in real time for air quality monitoring through tracking the fate and transport of pollutants generated from automobiles in highways considering the uncertainty of the system and demonstrate this capability for a case study in Atlanta, Georgia.

Air quality monitoring is essential for assessing the health impact of air pollutants. This is a complex problem, especially in the case of urban areas due to inhomogeneities in pollutant concentrations resulting from a multitude of emissions sources. One of the primary sources of pollutions is process industries. With the increased environmental regulations, emissions monitoring and management are critical to the process industry. An emerging area of data analytics and the industrial Internet of things (IIoT) for remote monitoring has been shown in Milward et al. (2019). Advanced applications using big data analytics are becoming popular among industrial sectors (Graessley et al. 2019). Information distribution using IIoT and big data analytics allows process industries to analyze data in real time and act promptly on failures. With a combination of UAS-based emission monitoring with process monitoring technologies, the process industry can utilize emission data along with their process data to reduce emissions for potential gain in adding value to the business (Vochozka et al. 2019). Similarly, cities can use dynamic sensing to provide timely advisories for the population.

The amount and the distribution of pollutants depend on the number of sources and the meteorology of the region. While the number and emissions intensity of sources determine the volume of the pollutants, it is the ground and upper layer airflow, temperature, humidity, sunlight, etc., that determine the fate and transport of the pollutant. The resulting concentrations of pollutants change spatially and temporally because of these physical and chemical processes. Due to the dynamic nature of the pollutant concentrations, static monitors are unable to detect the actual population exposure and are therefore unable to assess the actual impact of pollutants. The algorithm for optimal sensor placement should be robust enough that can dynamically locate sensors in real time to monitor the dynamic nature of air pollutants as well as consider the uncertainties associated with the system. This paper addresses the problem of minimizing the cost of

air pollution monitoring for evaluating health impact in the face of uncertainties.

The algorithm for dynamic sensor placement requires a time-series data of the distribution of pollutants in the region of interest for testing. Since traffic is the primary source of pollution in the urban area, we have considered pollutants from automobiles and their distribution for our case study. The objective is to determine the optimal locations of the sensors such that when combined with a comprehensive system model, the variability of the unmeasured variables can be minimized, thus maximizing observability by sensors. In the present problem, we are measuring pollutant concentrations based on the number of cars at strategic locations and dynamically placing a network of sensors so that the concentration of pollutants can be monitored. We can measure the observability of the sensor networks in terms of Fisher information (FI), which is a probabilistic function (Lee and Diwekar 2012). The spatiotemporal sensor positions in real time are solved as an optimization problem, solved for each time period. In this optimization problem, we have maximized the observability through maximizing FI subject to the fate and transport models of the pollutants under the weather as well as traffic uncertainty.

## Problem definition

As discussed earlier, emissions of pollutants from mobile sources like automobiles are uncertain in both time and space. Along with the location and time of emissions, the wind speed and other meteorological factors responsible for the fate and transport of pollutants are also uncertain. Optimal sensor placement in the present literature has not considered the inherent uncertainties in emissions and meteorological variables. The motivation behind this paper is to carry out stochastic optimization for real-time spatiotemporal sensor placement in the face of the uncertainties. A stochastic modeling capability of the AERMOD simulator developed in-house is implemented to capture the uncertainties in these variables and study their effects. AERMOD simulation software is originally developed by the United States Environmental Protection Agency (US EPA) (Fox 2017). This stochastic capability of AERMOD allows incorporating the uncertainty in source emissions as well as meteorological factors to predict distributions of pollutants. Along with the spatiotemporal distribution of the pollutants, we need to assess the population exposure in order to identify the optimal location of the sensors.

In this work, we have used a novel algorithmic framework based on the better optimization of nonlinear uncertain systems (BONUS) algorithm proposed by Sahin and Diwekar (2004) and the stochastic simulation capable modified version of AERMOD simulation software (Fox 2017) is used

to maximize the observability of the pollutants, in terms of both the spatiotemporal distribution and the population exposure in terms of intake in the face of uncertainties. To model the distribution of pollutants, we have used an advanced version of AERMOD developed at Vishwamitra Research Institute (VRI) that incorporates stochastic inputs in terms of both sources and meteorological data including wind speed and temperature, all of which are associated uncertainty.

## Application region and data collection

For the application of our algorithm, we have chosen an urban area with automobiles as the source of pollutants. The primary reason for this is the dynamics of the pollutants from automobiles, which has diurnal variations. The city of Atlanta has centers to count the number of automobiles at the prime location of the city, as can be found from the Georgia Department of Transportation's Traffic Analysis and Data Application (TADA) (2020). For our study, we have chosen the latitude and longitude of Atlanta (33.74 N and 84.38 W, respectively) as the center of the city. For convenience, we have considered the region between 33.64 N to 33.84 N in latitude and 84.28 W to 84.48 W in longitude as the region of interest. This area is shown in Fig. 1. It gives 0.2 degrees or 13.8 miles in latitude or  $y$ -axis and 11.5 miles in the longitude or  $x$ -axis.

In order to estimate the dispersion of pollutants, ten different automobile monitoring locations, as shown in Fig. 2, are used as the source of a pollutant for our study. The meteorological data for the city of Atlanta are obtained from the Georgia Environmental Protection Division (EPD 2020). The distribution of pollutants thus obtained is used to calculate the population exposure by considering the intake of the population of the region. Fisher information (FI) is estimated from both the concentration of pollutants and their intake. We have used the BONUS algorithm framework to optimize these decision variables, including the uncertainties to get our highest FI objective. In this work, we used data from 8 am to 5 pm (10 h). Thus, the diurnal changes are included in the problem. To our knowledge, there is no study on the dynamics of hourly spatial distribution of pollutants caused primarily by automobiles from the primary highways on the city of Atlanta, Georgia. Brantley et al. (2019) characterized spatial air pollution near the railyard area in Atlanta, Georgia. They have considered the emission primarily occurring within railyards that can affect nearby air quality. Mulholland et al. (1998), in their work, have assessed the temporal and spatial distribution of ozone in the Atlanta metropolitan area during the summer of 1993, 1994, and 1995. Thus, our present algorithm is unique that will give the flexibility to perform real-time spatiotemporal monitoring of pollutants and dynamic sensor placement.

**Fig. 1** Region of interest in Atlanta

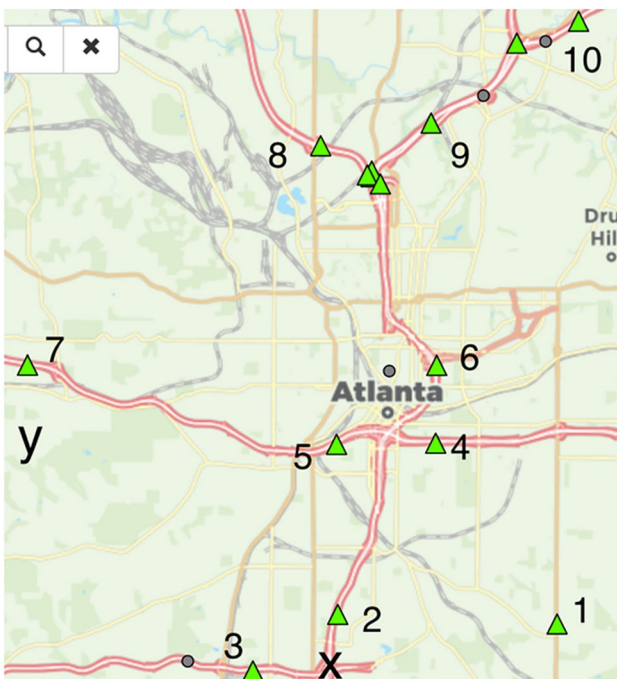
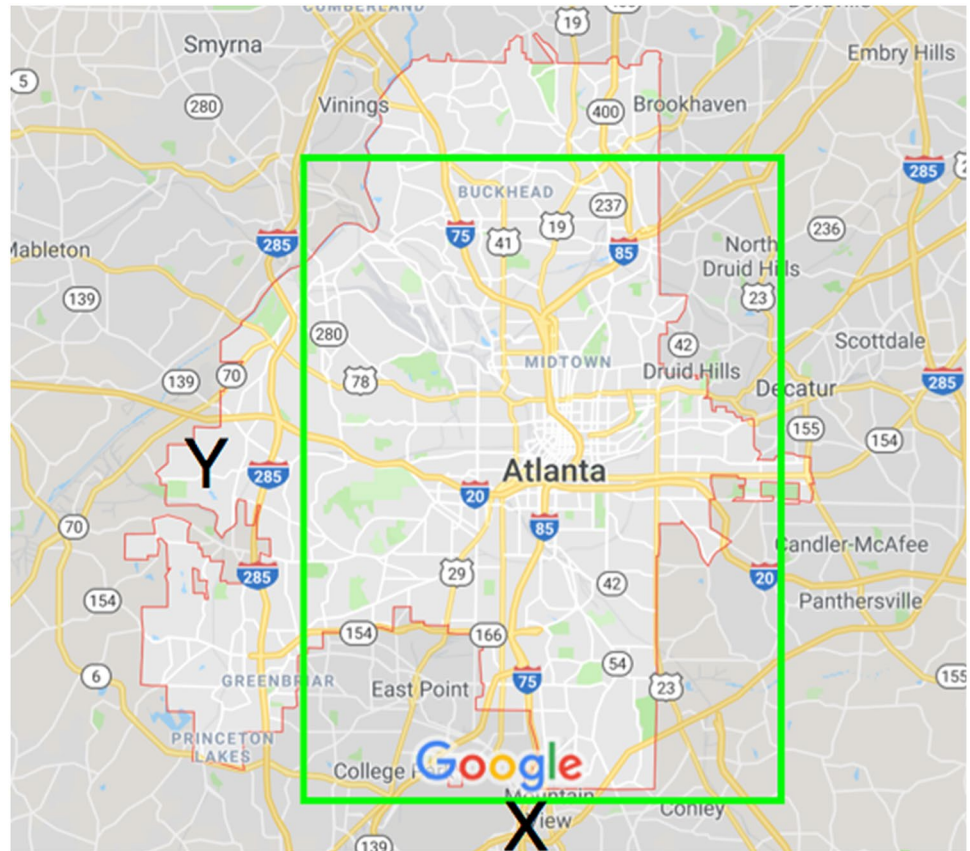


**Fig. 2** Pollutant source location in Atlanta. Ten different locations (as numbered) are chosen: Map© Thunderforest

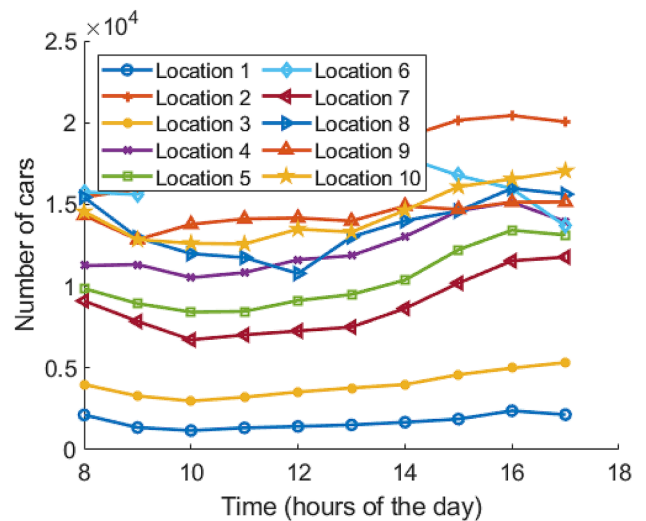


**Fig. 3** Flow diagram to find optimal sensor location with optimizing FI

**Uncertainties in pollutant distribution system**

At any given time (h) of the day, the mean number of vehicles is given in Fig. 3. On different days, the number of vehicles is assumed to vary with a normal distribution around the

mean. The  $3\sigma$  of the distribution is assumed to be  $\pm 5\%$  of the mean. There are uncertainties associated with meteorological data as well. Meteorological data are also assumed to vary at different days with  $3\sigma$  of the distribution assumed to be  $\pm 5\%$  of the mean. From the distribution, 100 samples are generated. The stochastic version of AERMOD developed in-house is used to estimate the pollutant concentrations at different spatial locations for each sample point. The average pollutant concentration is generated using the average from 100 samples. The process is repeated for each hour.

Although uncertainty is inherent in pollution fate and transport models, it does not receive much attention in the literature. Monitoring urban air pollution is a challenging task. Recently, Moltchanov et al. (2015) studied the feasibility of measuring urban air pollution by wireless, distributed sensor networks. Air pollution monitoring using a sensor grid environment is shown by Ma et al. (2008). They have provided an optimal node organization to obtain homogeneous sensor data. Grid-based monitoring of air pollution data has also been performed by Richards et al. (2006). Mobile and wireless sensor networks and real-time monitoring technology of air pollution are relatively recent. Marjovi et al. (2015) have generated air pollution maps using mobile sensor networks. The significance of real-time monitoring using wireless sensor networks is shown by Kadri et al. (2013). Recently, Kaivonen and Nagi (2020) showed the same by using sensors on city buses. Mihăiță et al. (2019) have shown the effectiveness of combined stationary and smart mobile pollution monitoring for air quality evaluation using data-driven modeling. Reis et al. (2015) have shown integrating modeling and smart sensors for human exposure monitoring. However, none of these papers address the problem of optimization for real-time spatiotemporal sensor placement in the face of weather and source uncertainties. This is the focus of the current endeavor.

## Problem formulation

In the sensor placement problem, the objective is to determine the optimal locations for a network of sensors such that when combined with a comprehensive system model, the variability of the unmeasured variables can be minimized, thus maximizing observability (Diwekar 2008). We can measure observability in terms of Fisher information, FI of pollutant concentrations as a probabilistic function. We can also measure observability in terms of Fisher information of the variable population exposure. These are both probabilistic functions. As the problem involves probabilistic objective function and uncertainties, the problem can be classified as a stochastic optimization problem.

Since we are determining spatiotemporal positions of the sensors, this is also a real-time optimization solved for each

time period. The number of sensors is linked to the performance and error characteristics of sensors, and further, virtual sensing (model-based) has its own error characteristic. In the absence of a hardware sensor, this characteristic is used along with fate and transport models (virtual sensing). If no cost data are available, then we can limit the maximum number of sensors. Here, we assumed a maximum number of sensors and converted this problem into a stochastic nonlinear programming problem using  $x$  and  $y$  coordinates of the sensor positions. The following stochastic optimization problem is solved for different numbers of sensors at different hours of the day.

$$\max_{x_i, y_i} \sum_{i=1}^n FI_i(x_i, y_i) \quad (1)$$

$$\begin{aligned} \text{Subject to: } n &\leq n_{\max} \\ \text{Distance between sensors} &\leq d_{\min} \end{aligned} \quad (2)$$

and

AERMOD models with exposure assessment models.  
Weather and model uncertainties.

where  $n$  is the number of sensors,  $FI_i$  ( $i = 1, 2, \dots, n$ ) is the FI for process variable,  $n_{\max}$  is the maximum number of sensors allowed, and  $B$  is the total sensor budget. By determining the spatiotemporal placement of sensors over all measurable process variables by using objectives like FI and cost as metrics for optimization, the overall number of sensors can be reduced, thereby producing an effective and efficient spatial-temporal sensor network.

## Objective function for the problem

Different pollutants that need to be considered for assessment (from automobiles) include  $\text{NH}_3$ ,  $\text{NO}_x$ ,  $\text{SO}_x$ , volatile organic compounds (VOCs), and carbon graphite as particulate matter (PM). The human exposure assessment requires two steps for converting the pollutant concentration into human exposure Baratto et al. (2005). These are:

- data collection and analysis;
- exposure assessment;

Data collection is to gather site-specific data, which include site characteristics to identify potential pollutant pathways and exposure points as well as other data needs for modeling purposes. The site-specific data depend on the land use category. In the present problem, we have considered the Atlanta City region to model the fate and transport of the pollutants. The exposure assessment is performed based on the amount of toxicant on the population. The concentration of a toxicant and the population at any particular site is used to calculate net exposure ( $Ex$ ) at the given site. It is given as:

$$Ex = C \times P \tag{3}$$

where the net exposure is  $Ex$  ( $\text{mg}/\text{m}^3$ ),  $C$  is the average concentration contacted over the exposure period ( $\text{mg}/\text{m}^3$ ), and  $P$  is the population.

We are considering Fisher information as the measure of observability of sensors. The calculation of Fisher information from the concentration, as well as exposure data, is given below:

For a given random variable  $X$ , the probability distribution, which depends on an unknown parameter  $\theta_x$ , is given by the continuous likelihood function ( $f_{X,\theta_x}(X|\theta_x)$ ). In order to estimate the unknown parameter  $\theta_x$ , it is essential to capture the observability of  $\theta_x$ , i.e., variability of the observations. Fisher information (FI) is a measure of observability that can be used to indicate the accuracy of the uncertainty estimation. Through FI, we can capture the amount of information that the set of observations contains about the parameter  $\theta_x$ . Unlike Shannon information, which is a global measure of the occurrence of  $\theta_x$ , FI can be used as a local metric of observability.

FI is defined as: Given a random variable  $X$  and its associated density function ( $f_{X,\theta_x}(X|\theta_x)$ ) which depends on the parameter vector  $\theta \in \Theta$ , and  $\theta_x$  is the  $x^{\text{th}}$  component of  $\theta$ , the Fisher information associated with  $\theta_x$  is Rico-Ramirez et al. (2010):

$$FI_{\theta_x} = \int \frac{1}{(f_{X,\theta_x}(X|\theta_x))} \left( \frac{\partial(f_{X,\theta_x}(X|\theta_x))}{\partial\theta_x} \right)^2 dX. \tag{4}$$

Due to the gradient operator  $\frac{\partial}{\partial\theta_x}$ , FI measures the amount of change in the likelihood function due to a change in the unknown parameter value  $\theta_x$ . Lower FI indicates that  $f_{X,\theta_x}(X|\theta_x)$  changes slower with respect to a change in  $\theta_x$ , which corresponds to lower observability in regards to estimating the true parameter value and vice versa.

In this problem, we have a single measured variable which is the concentration of pollution ( $x$ ) in the given region that changes with time due to uncertainties in the volumes of automobiles at different time as well as with meteorology. (In case of Fisher information for exposure, this variable is replaced by  $Ex$  given in Eq. 3.) The parameter to be estimated is the mean value of pollutant ( $a$ ). The probability density function  $f_{X,a}(X|a)$  with respect to the true value of the variable is given as follows:

$$FI_a = \int \frac{1}{(f_{X,a}(X|a))} \left( \frac{\partial(f_{X,a}(X|a))}{\partial a} \right)^2 dX. \tag{5}$$

The calculation of FI requires the determination of its probability density function (PDF). To have a continuous distribution for which derivative can be estimated, we use Kernel density estimation to generate the PDF information.

(For details, please refer to Diwekar and David (2015).) FI captures the changes in distribution and can provide a good measure for the observability of a variable.

### The BONUS algorithm for stochastic optimization

In the presence of uncertainties, an optimization problem is converted into stochastic optimization. The objective function is probabilistic in nature. Sometimes, the constraints can also be probabilistic as well. A generalized stochastic optimization problem can be represented as follows:

$$\text{Optimize } P_1(Z(x, u)) \tag{6}$$

$$\begin{aligned} \text{subject to } P_2(h(x, u)) &= 0 \\ P_3(g(x, u)) &\geq 0 \end{aligned} \tag{7}$$

where  $P$  represents the cumulative distribution functional such as the expected value, mode, variance or fractiles and  $u$  is the uncertain variables expressed in terms of probability distributions. In our problem, we use the expected value of the objective function. Depending on the type of optimization, stochastic optimization problems can be further classified as stochastic linear programming, stochastic nonlinear programming, and stochastic mixed integer linear and nonlinear programming problems. Our problem is a stochastic nonlinear programming problem as the system is nonlinear, and decision variables are continuous scalar variables.

There are two fundamental approaches used to solve stochastic nonlinear programming (SNLP) problems. The first set of techniques identifies problem-specific structures and transforms the problem into a deterministic nonlinear programming (NLP) problem. For instance, chance-constrained programming (Charnes and Cooper 1959) replaces the constraints that include uncertainty with the appropriate probabilities expressed in terms of moments. The major restrictions in applying the chance-constrained formulation include the following: The uncertainty distributions should be stable distribution functions, the uncertain variables should appear in the linear terms in the chance constraint, and the problem needs to satisfy the general convexity conditions. The advantage of the method is that one can apply the deterministic optimization techniques to solve the problem. Decomposition techniques like L-shaped decomposition (Birge and Louveaux 1997) divide the problem into stages and generate bounds on the objective function by changing decision variables and solving subproblems that determine the recourse action with respect to the uncertain variables. However, these methods also require convexity conditions and/or dual-block angular structures and are only applicable to discrete probability distributions. Examples of this include the Lagrangian-based approaches like the regularized decomposition technique (Ruszczynski 1986) and the

progressive hedging algorithm (Rockafellar and Wets 1991) used for SNLP problems. These methods have limitations in terms of handling uncertain variables as the number of scenarios considered tend to be small.

An alternative approach that can be used to capture uncertainty is through a sampling loop that is embedded within the optimization iterations for the decision variables, as shown in Fig. 4.

Figure 4 represents the general calculation sequence for any stochastic optimization problem (Diwekar and David 2015). From Fig. 4, the inner loop finds a probabilistic representation of the objective function and constraints using the sampling loop or scenario loop. The outer optimization loop determines the decision variables. For these decision variables at each iteration, a sample set or scenario set of uncertain variables is generated, and the model is run for each of these sample (scenario) points. The value of the probabilistic objective function and constraints is calculated. For nonlinear programming problems, the derivative information is also needed, which is again calculated by perturbation of each decision variable using the sampling loop or scenario loop for each perturbation. This is a computationally expensive procedure making these methods ineffective for even moderately complex models.

Better optimization of nonlinear uncertain systems (BONUS) algorithm was proposed by Sahin and Diwekar (2004) to circumvent this problem. In BONUS, the inner sampling loop with sample model runs (Fig. 4) is only used for the first iteration. In this first iteration, the decision variables are assumed to have uniform distributions (between upper and lower bounds). Specified probability distributions of uncertain variables together with uniform distribution of decision variables form the base distributions for analysis. The solution space of the objective function and constraints

is obtained by sampling only at the base distribution at the beginning of the analysis. As the optimization proceeds, the decision variables change, and the underlying distributions for the objective function and constraints transform. A reweighing scheme is used based on the ratios of the probabilities for the current, and the base distributions to find the values of objective function and constraints. A schematic diagram of the reweighing scheme is shown in Fig. 5. To have a smooth function for the probabilities, we approximate the distributions using kernel density estimation techniques. For details about the BONUS algorithm, please refer to Diwekar and David (2015).

In this problem, we have used the Hammersley sequence sampling (HSS) of the Fisher information (FI) for the initial base distributions. HSS is an efficient sampling technique developed by Diwekar and co-workers (Diwekar and Kalagnanam, 1997). HSS has been used for various applications in order to improve the efficiency of simulations (Diwekar and Ulas 2007). It uses Hammersley points to uniformly sample a unit hypercube and invert these points over the cumulative probability distribution to provide the sample set for the variable. This enables the sampling to be uniformly distributed in n-dimensions that are not achievable by pseudo-random sampling, as shown by Mukherjee and Diwekar (2016) in the optimal spatial configuration of a polymer solution. The algorithm we have developed is essentially a sequential quadratic programming (SQP) algorithm that uses the reweighing scheme to estimate objective function and gradient at each iteration instead of the sampling loop. The Hessian is approximated by using the Broyden–Fletcher–Goldfarb–Shanno (BFGS) formula.

The general procedure involves the following two steps. Since we need expected value for objective function and constraint for this problem, the procedure is described in terms of expected value calculations.

1. *Off-line Computations* (Generating base distributions and objective function data from AERMOD): Draw independently distributed samples  $j = 1, \dots, N_{\text{samp}}$  for uncertain variables  $u$  and decision variables  $x$  (FI in the present problem). The distributions for the decision variables are assumed to be uniform distributions between upper and lower bounds of the decision variables. Use these samples to generate the design prior density function  $P^p(x, u)$  using kernel density estimation (KDE). Evaluate the objective function  $Z$  (and the probabilistic constraint) for each sample.
2. *Online Computations* (Using BONUS reweighing scheme to solve the sensor placement problem shown in Eqs. 6 and 7).

- (a) At each iteration  $k$ , the decision variables  $x^k$  (in the first iteration, the initial value of decision vari-

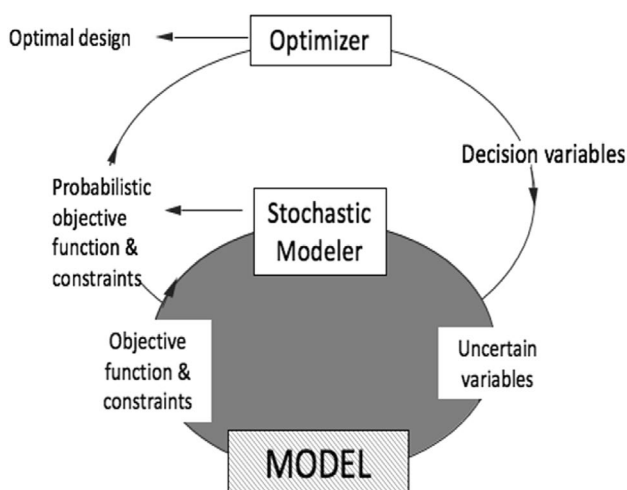


Fig. 4 Percentage of eyes with SRF resolved versus persistent among different visits for the whole sample

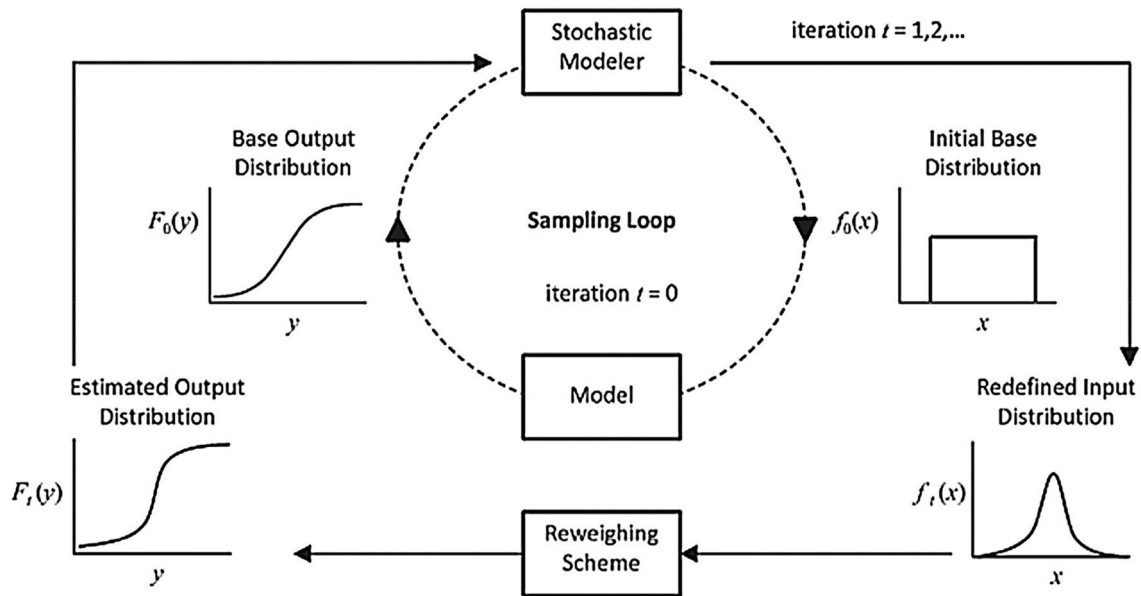


Fig. 5 BONUS reweighting approach (Lee and Diwekar 2012)

ables is given) define a narrow normal distribution around this point (Fig. 5) and draw samples of  $x^k$  from it. Use samples to generate the design distribution  $P^d(x, u)$  using KDE. Estimate the objective function and constraint (expected value  $E$ ) using the following the reweighting formula:

$$V(x^k) = E((x, u)) = \sum_{j=1}^{Nsamp} \omega_j^k Z(x^k, u) \tag{8}$$

where

$$\omega_j^k = \frac{P^d(x_j^k, u) / P^p(x_j^k, u)}{\sum_{ij=1}^{Nsamp} P^d(x_{ij}^k, u) / P^p(x_{ij}^k, u)} \tag{9}$$

and satisfy

$$\sum_{j=1}^{Nsamp} \omega_j^k = 1. \tag{10}$$

- (b) Perturb the decision variable  $x^k$  and use the reweighting scheme to estimate  $V(x^k + \delta x^k)$ . Find the gradient and KKT conditions. If KKT conditions are satisfied, terminate, go to step 2,c.
- (c) SQP computation: Use gradient to compute the Hessian approximation  $H^k$  using BFGS formula and compute step  $\Delta x$  for decision variables by solving the quadratic program (QP):

$$\min_{\Delta x} \nabla V(X^k)^T \Delta x + \Delta x^T H^k \cdot \Delta x \tag{11}$$

$$s.t. X^k + \Delta x \tag{12}$$

Cut the step if necessary to obtain a new iterate  $x^{k+1} = x^k + \alpha \Delta x$  with  $\alpha \in (0,1)$ .

- (d) Go to step 2.a.

The solution space consists of multiple local optima. This can be observed as we change the initial values of the decision variables ( $x, y$  coordinates of sensors). To cover the space uniformly, we have used Latin hypercube Hammersley sampling to generate the initial values. The best solution is picked by the one with the highest FI. Figure 6 provides the program structure.

The steps for the solution of the spatiotemporal sensor placement problem are shown in Fig. 7.

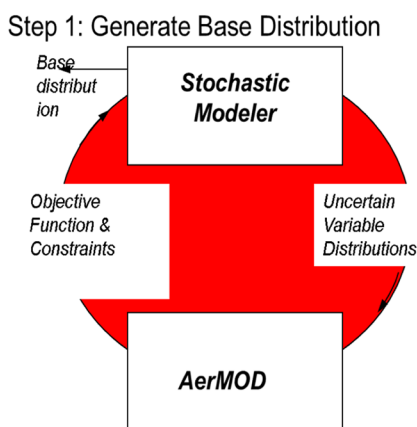
### Results and discussion

In the present work, our goal is to understand the distribution of pollutants as well as their exposure to the human population in the city of Atlanta. The time-series distribution of pollutants for diurnal fluctuation of the number of automobiles, wind speed, and temperature are presented in this work. The mean number of vehicles at each counting station at a different time, as used in the present work, is shown in Fig. 3.

SO<sub>2</sub> and carbon graphite, as particulate matter 2.5 (PM), are considered for our analysis. The source of pollution is considered as a point source. The release of pollutants per location is considered to be 1.00E-03 g/s and 2.20E-04 g/s



**Fig. 6** Calculation sequence for optimal sensor placement with the AERMOD model and BONUS algorithm



**Step 2. Optimize for sensor placement**

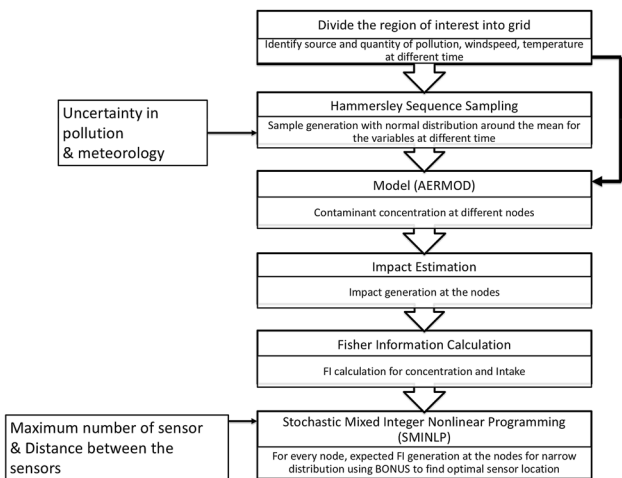
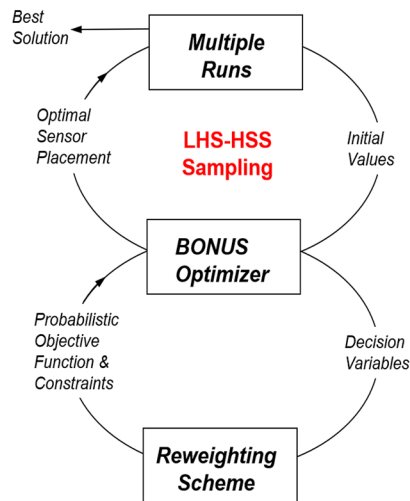


**Fig. 7** Flow diagram to find optimal sensor location with optimizing FI

per vehicle for SO<sub>2</sub> and PM, respectively. The exhaust is assumed to be at the height of 1 m from the ground. The exit temperature is assumed to be 425 K. The velocity of the exhaust is assumed to be 1 m/s, and the diameter of the exhaust is assumed to be 0.1 m. Urban effects and the urban area are applied to each source. Since a gross assumption is made for the source of pollution, our goal is to find the impact of airflow (both surface and upper layer) on the average distribution of pollutants over the city of Atlanta. It is to be mentioned that the topography of Atlanta has not been included in the AERMOD model. However, the contribution of the paper is to provide an efficient way of finding real-time sensor placement for a city, and the problem uses sufficient information to provide the required output.

To find the distribution of pollutants within the region, the region of interest in the city of Atlanta is divided into grids as shown in Fig. 8. Figure 8 also shows the distribution of the population in different neighborhoods of Atlanta. Ten different location are identified as sources of pollutants, as shown in Fig. 2. The pollutants are monitored for 10 h, starting from 8 am to 5 pm. Along with diurnal variation, there is a variation on different days of the year. Pollution source, wind speed, and temperature uncertainty will vary with mean  $\mu$  and standard deviation  $\sigma$  (spread  $\mu \pm 3\sigma$ ). It is assumed to vary  $\pm 5\%$  of the mean. Simulation is performed with two different methods:

- (A) Maximizing FI as obtained from pollution distribution
- (B) Maximizing FI as obtained from exposure of pollutant on human population

The exposure assessment for each node is obtained using the average concentration of the population at the neighborhood where the node is located. Exposures are calculated from the amount of chemical at the exchange boundary (e.g., skin, lungs, gut) and available for absorption to the human body. It is given as:

$$Ex_i = C_i \times P_i \tag{13}$$

$Ex_i$ : net exposure at node  $i$  ( $g/m^3$ ),  $C_i$ : average concentration contacted over the exposure period at node  $i$  ( $g/m^3$ ), and  $P_i$ : the population at the node  $i$ . Figure 9 shows the distribution of FI at different times from the concentration of PM, and Fig. 10 shows the FI from exposure from the distribution of PM.

**Fig. 8** Population distribution in different neighborhoods of Atlanta: Map © Cedar Lake Ventures, Inc.

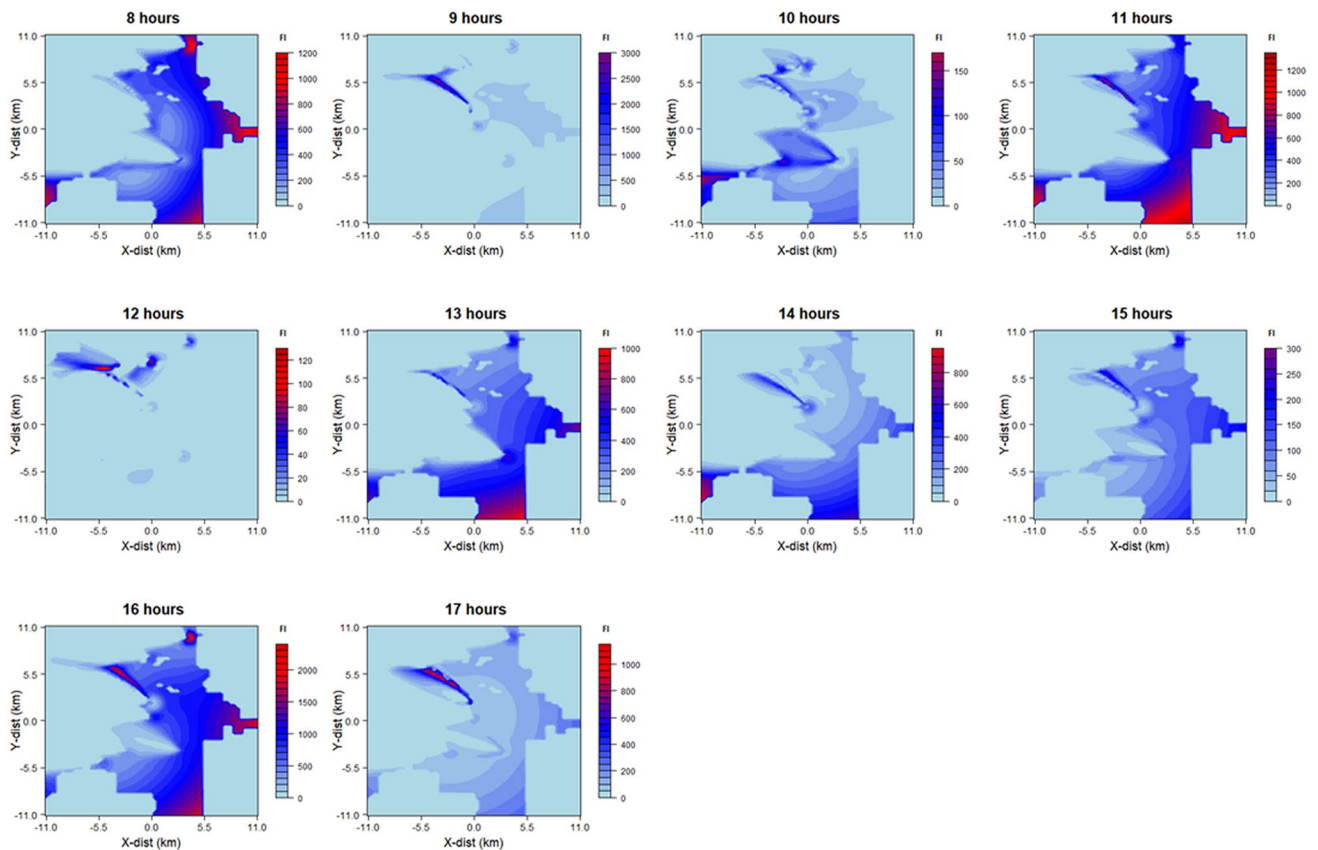
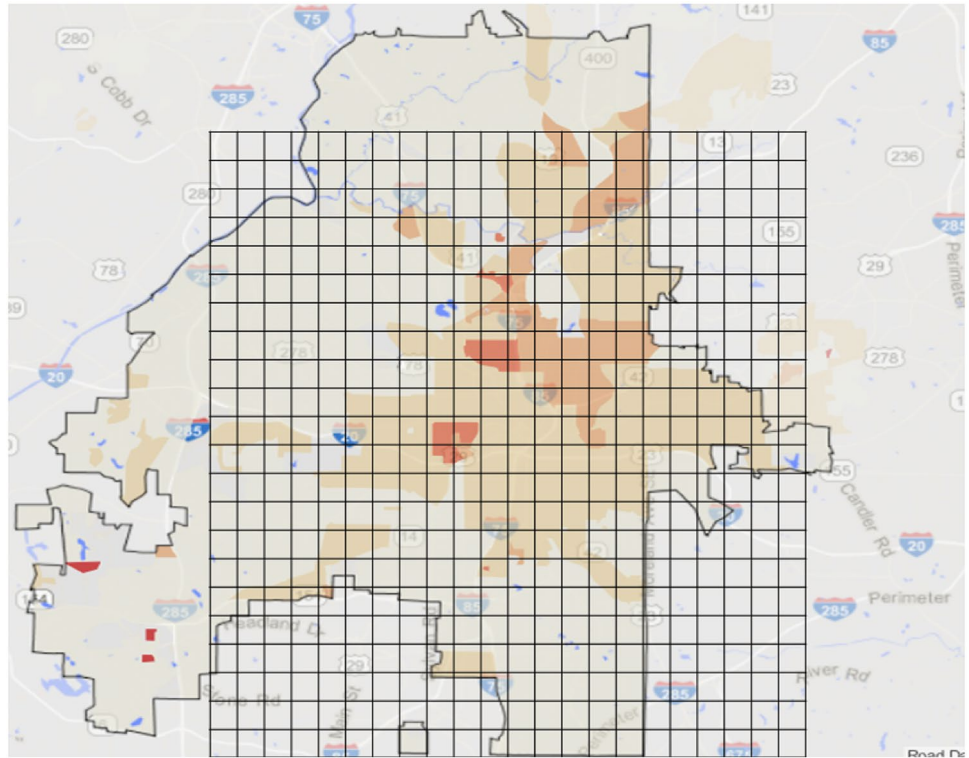


**Fig. 9** Distribution of FI at different times from the concentration of PM. The x and y coordinates represent the distance from the center of the city as shown in Figure 1, and the color represents the intensity of FI

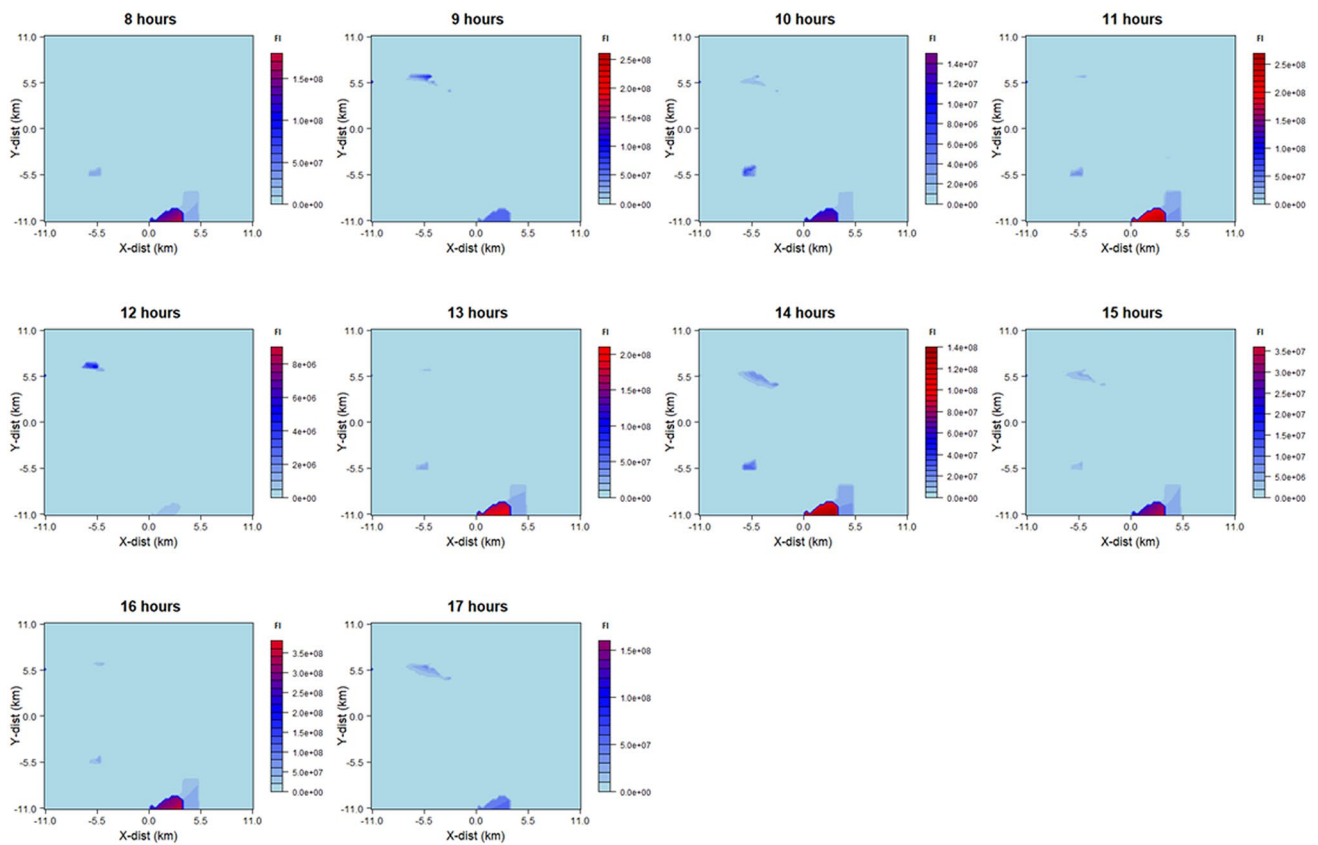


**Fig. 10** Distribution of FI at different times from the exposure of PM. The x and y coordinates represent the distance from the center of the city as shown in Figure 1, and the color represents the intensity of FI

In BONUS, the first step is to generate our base sample set. We have identified 12 uncertain variables: wind speed, temperature, and the number of automobiles at the ten locations. Hundred samples of these 12 variables are generated using HSS. Decision variables are assigned a normal distribution with their upper and lower bounds specified. The mean value of the output information from AERMOD at each time is used to estimate the FI, which defines the objective function. BONUS is then used to find the optimal solution of sensors for all 10 h. It has been found that the stochastic nonlinear problems are non-convex. The solution space consists of multiple local optima. This can be observed as we change the initial values of the decision variables ( $x, y$  coordinates of sensors). To avoid getting trapped in local solutions, we provided ten different initial values for the algorithm. These different initial values needed different iterations to get to the optimum. Figure 11 presents multiple solutions using ten different initial values of decision variables.

To cover the space uniformly, we are using Latin hypercube Hammersley sampling to generate the initial values. Table 1 presents the multiple solutions as obtained from different initial values, also shown in Fig. 12. The objective

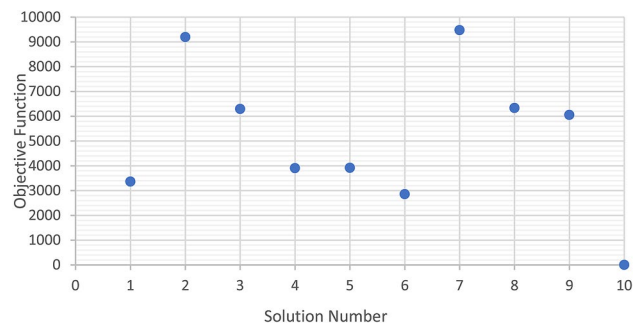


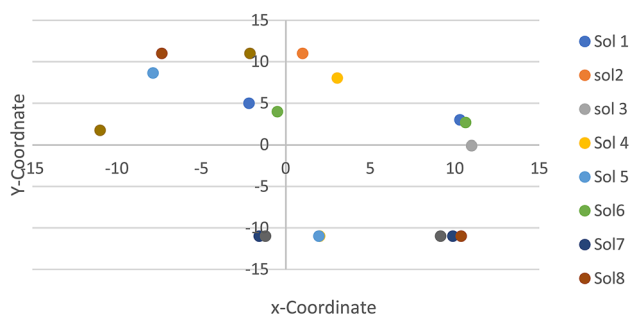
**Fig. 11** Optimal objective function values for multiple optimization runs

function here is FI based on exposure for a particular day in Atlanta at 8 AM. We can see from Fig. 11 that the best solution is solution 7 with the highest FI. The sensor positions for this solution are shown in Fig. 12. We had given a constraint that the sensors should be at least 10 km apart. Since this is an NLP problem, we used Karush–Kuhn–Tucker (KKT) error (optimality criteria) for stopping criteria (Diwekar 2008). The tolerance for KKT error is set to 1.00E−03% of the objective function value.

**Table 1** Solutions from different initial values for decision variables

Run no.	Sensor 1, X	Sensor 1, Y	Sensor 2, X	Sensor 2, Y
1	9.21	-1.80	3.30	6.16
2	8.54	5.02	-3.99	0.73
3	5.45	-8.21	8.80	-1.00
4	3.05	7.96	2.00	-4.86
5	1.96	-6.06	-8.92	8.37
6	-0.21	3.78	5.30	3.04
7	-4.00	-9.60	-6.41	-10.56
8	-4.92	9.67	-7.85	-8.48
9	-8.56	-4.10	9.01	-4.24
10	-11	1.73	-2.13	10.96

Optimal Sensor Placement: Multiple Solutions

**Fig. 12** Optimal sensor placement for Atlanta, Georgia, using Fisher information (FI) based on particulate matter (PM) concentration, at different hours of the day. The  $x$  and  $y$  coordinates represent the distance from the center of the city as shown in Fig. 1, and the color represents the intensity of FI

We solved the problem for two sensors located at a minimum distance of 10kms apart for different hours. Figure 13 shows the FI distribution at different hours of the day. It can be seen that the distribution changes significantly due to different traffic conditions throughout the day. The positions of the two sensors (marked by yellow stars) are selected based on maximum FI without fail for all conditions. Since the distributions are different, the sensor positions also change accordingly.

## Results based on population exposure

Figure 14 shows the FI distribution at different times of the day when the pollutant's exposure to the population is accounted for along with the position of the sensor. In this case, also, the sensors are optimally placed where the impact is maximum. Since the minimum distance between the two sensors is specified at 10 kms, it does not put sensors closer where the impact can be higher. It can be seen that the sensor

positions are different as obtained from FI based on concentration. In this case, the impact is higher where concentration and population are both high.

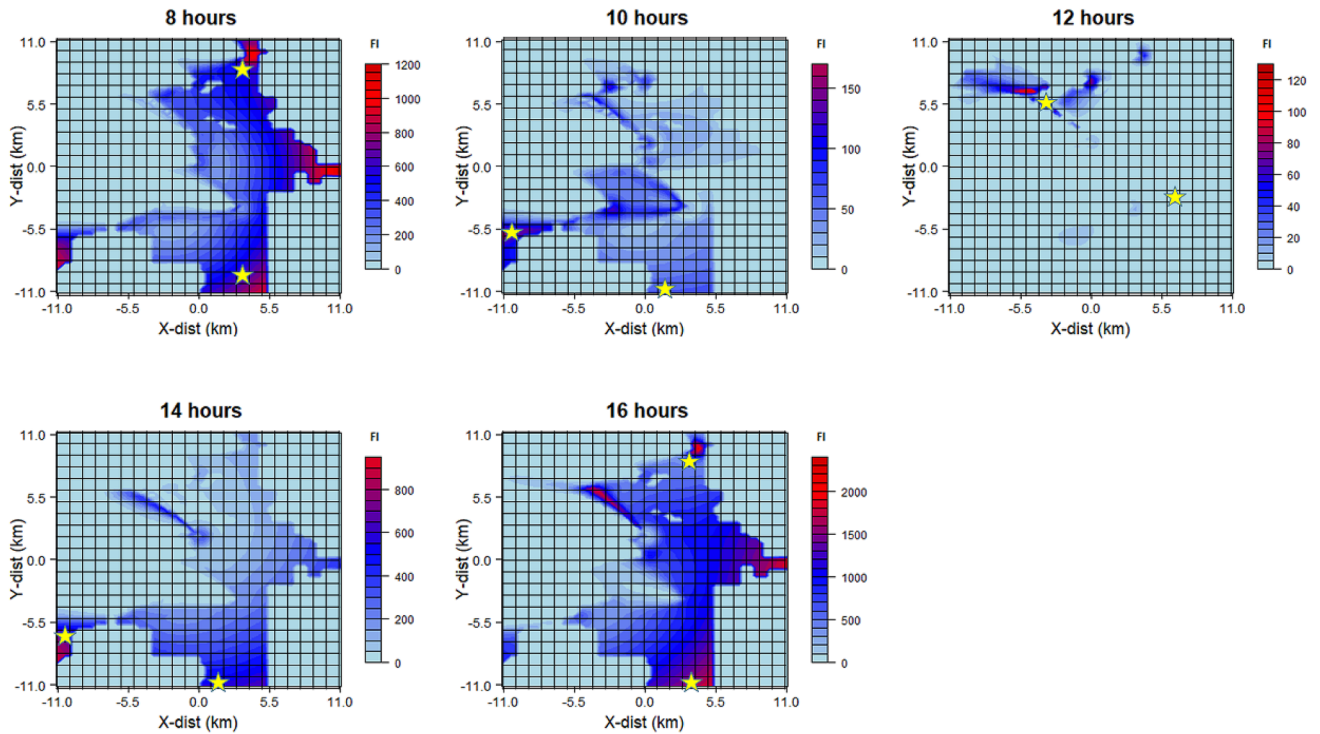
It is expected that as we dynamically move the sensor, we are able to capture more information. Table 2 shows the percentage increase in information by dynamically moving the sensor by comparing the information at optimal location with that from a static sensor position as at 8 h.

It is also expected that as we increase the number of sensors, we can capture more information. An analysis is performed to see the impact of the increased number of sensors. Figure 15 shows the change in optimum objective values as we increase the number of sensors from 2 to 10 at 8 a.m.

## Conclusions and future work

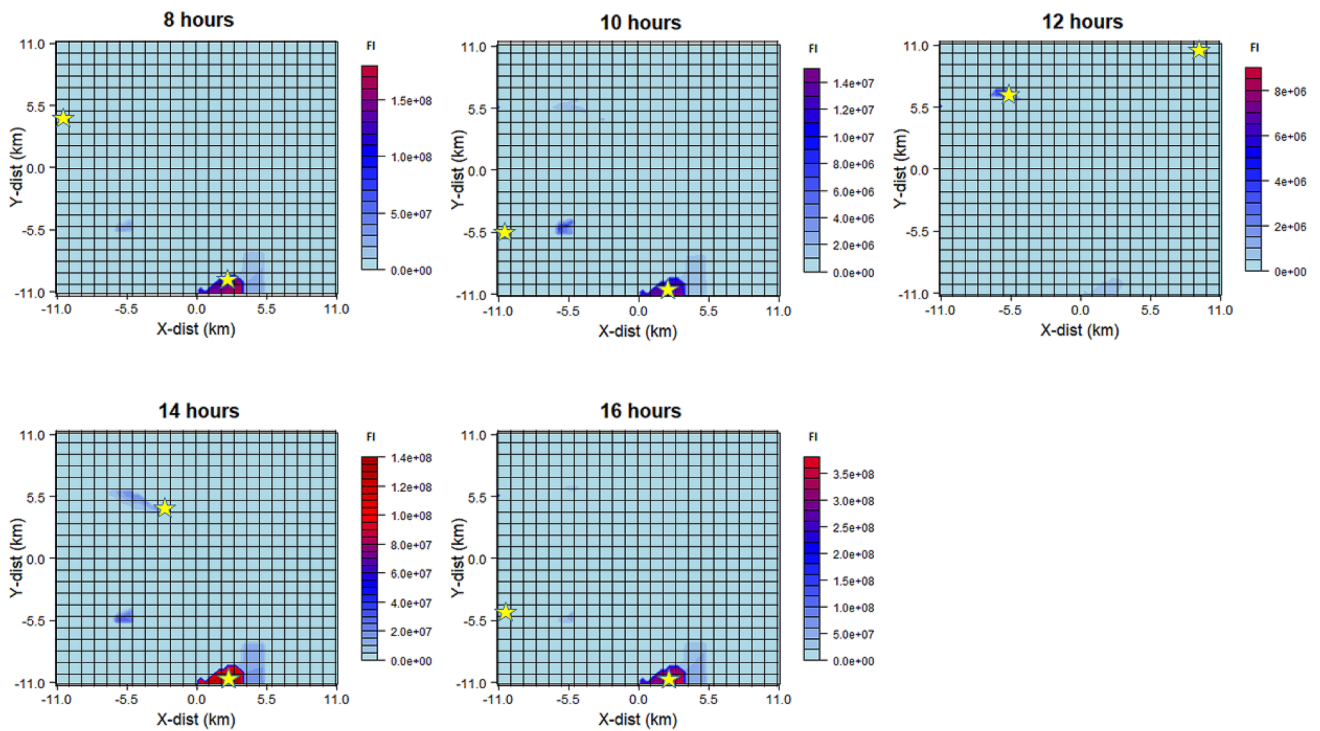
This is the first-time algorithm developed to carry out real-time spatiotemporal sensor placement for air pollution monitoring. Also, for the first-time, weather uncertainties are included in real-time sensor placement for air pollution monitoring. A real-world case study for the city of Atlanta, Georgia, is presented. Real-time spatiotemporal sensor placement problem is solved by stochastic optimization method using the BONUS algorithm, considering uncertainty in pollutant sources as well as meteorology. Results from the intake formulation (B) (population exposure) are significantly different from that of method A (pollutant concentration alone). Comparing methods A and B, we can say that consideration of pollution intake of the population affects the choice of sensor nodes. When we compare quantitative gain due to dynamic sensing as compared to fixed sensors, we found that the information increase due to dynamic sensing is 3–134 times that of static sensors. BONUS reweighting scheme has made the present method computationally efficient to solve it in real time. Dynamic sensing with portable low-cost sensors is a new area for monitoring, which shows promise for exposure assessment. This paper provides a novel theoretical basis for such an endeavor. BONUS algorithm provided optimal solutions to the sensor placement under weather and pollutant source uncertainties for the city of Atlanta in a real time. Unlike stationary monitoring stations, our real-time sensor placement optimization algorithm will allow, for the first time, the assessment of spatial–temporal variability of pollution.

Recently, US government approved regulations for the use of commercial drones. Theories and framework developed in this work will also be useful for drone-based monitoring. Our method is also going to be useful in drone-based monitoring of water bodies, water security networks, and sensor placement for advanced power systems with similar applications to other infrastructure issues like security of the power grid, a possibility. This work demonstrated the



**Fig. 13** Optimal sensor placement for Atlanta, Georgia, using Fisher information (FI) based on particulate matter (PM) concentration, at different hours of the day. The  $x$  and  $y$  coordinates represent the dis-

tance from the center of the city as shown in Fig. 1, and the color represents the intensity of FI

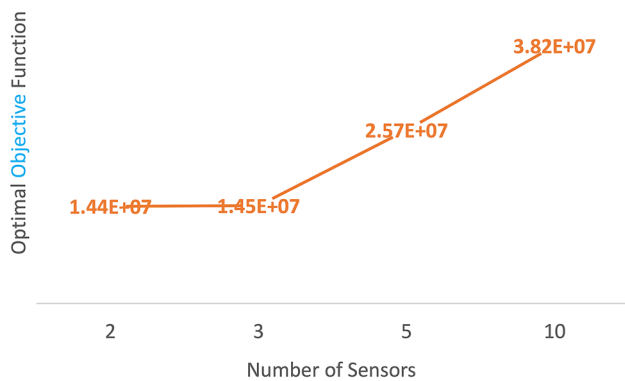


**Fig. 14** Optimal sensor placement for Atlanta, Georgia, using Fisher information (FI) based on exposure from particulate matter (PM), at different hours of the day. The  $x$  and  $y$  coordinates represent the dis-

tance from the center of the city as shown in Fig. 1, and the color represents the intensity of FI

**Table 2** Percentage improvement in information acquisition by dynamically moving the sensor at optimal location

	Time	Maximum FI	FI from static location optimal at 8 hrs	% increase in information
Analysis with concentration	8 h	-1.83E+03		
	10 h	-2.12E+02	-5.22E+01	306.13
	12 h	-8.51E+01	-1.93E+00	4309.33
	14 h	-1.39E+03	-5.06E+02	174.70
	16 h	-3.49E+03	-1.45E+03	140.69
Analysis with exposure	8 h	-1.44E+07		
	10 h	-1.20E+06	-5.42E+05	121.40
	12 h	-3.10E+05	-2.83E+03	10854.06
	14 h	-1.24E+07	-1.42E+06	773.24
	16 h	-2.83E+07	-2.09E+05	13440.67

**Fig. 15** Optimal objective values for different numbers of sensors at 8 h

applicability of the stochastic optimization method using the BONUS algorithm for dynamic sensor placement. More work is needed to show the robustness of the method by simulating the fate and transport of pollutants for a longer time period (weeks to months). In addition, one could evaluate the technique for multiple sources of pollutants instead of just the automobile sources, as was done for this initial demonstration.

**Acknowledgements** The work is funded by a grant from Electric Power Research Institute (EPRI) (Grant No. EP-10010252). The views expressed in this paper are those of the authors and do not necessarily represent the view of EPRI.

## References

Baratto F, Diwekar UM, Manca D (2005) Impacts assessment and tradeoffs of fuel cell based auxiliary power units: part II. Environmental and health impacts, LCA, and multi-objective optimization. *J Power Sources* 139(1–2):214–222.

- Berry JW, Fleischer L, Hart WE, Phillips CA, Watson JP (2005) Sensor placement in municipal water networks. *J Water Resources Plan Manag* 131(3):237–243
- Birge JR, Louveaux F (1997) Introduction to stochastic programming. Springer, New York
- Brantley HL, Hagler GS, Herndon SC, Massoli P, Bergin MH, Russell AG (2019) Characterization of spatial air pollution patterns near a large Railyard area in Atlanta, Georgia. *Int J Environ Res Public Health* 16(4):535
- Charnes A, Cooper WW (1959) Chance-constrained programming. *Manage Sci* 6(1):73–79
- Dantzig GB, Infanger G (1991) Large scale stochastic linear programs—importance sampling and Bender decomposition. In: Brezinski C, Kulisch U (eds) Computational and applied mathematics, pp 111–120
- Diwekar U, Ulas S (2007) Sampling techniques, Kirk-Othmer Encyclopedia of chemical technology, Online Edition 26:998
- Diwekar UM, David A (2015) BONUS algorithm for large scale Stochastic nonlinear programming problems. Springer, Heidelberg
- Diwekar UM, Kalagnanam JR (1997) Efficient sampling technique for optimization under uncertainty. *AIChE J* 43(2):440–447
- Diwekar UM (2008) Introduction to applied optimization. Springer, New York
- Diwekar UM, Mukherjee R (2017) Optimizing spatiotemporal sensors placement for nutrient monitoring: a stochastic optimization framework. *Clean Technol Environ Policy* 19(9):2305–2316
- EPD (2020) The Environmental Protection Division (EPD) of the Georgia Department of Natural Resources <https://epd.georgia.gov/air-protection-branch-technical-guidance-0/air-quality-modeling/georgia-aermet-meteorological-data>. Accessed 12 May 2020
- Fox T (2017) EPA White Papers on Planned Updates to AERMOD Modeling System. <https://www.epa.gov/scram/aermod-modeling-system-development>. Accessed 12 May 2020
- Graessley S, Suler P, Klietk T, Kicova E (2019) Industrial big data analytics for cognitive internet of things: wireless sensor networks, smart computing algorithms, and machine learning techniques. *Anal Metaphys* 18:23–29
- Higle JL, Sen S (1991) Stochastic decomposition: an algorithm for two-stage linear programs with recourse. *Math Oper Res* 16(3):650–669
- Jácome G, Valarezo C, Yoo C (2018) Assessment of water quality monitoring for the optimal sensor placement in lake Yahuarcocha using pattern recognition techniques and geographical information systems. *Environ Monit Assessment* 190(4):259
- Kadri A, Yaacoub E, Mushtaha M, Abu-Dayya A (2013) Wireless sensor network for real-time air pollution monitoring. In: 2013 1st

- International conference on communications, signal processing, and their applications (ICCSPA), IEEE, pp 1–5.
- Kaivonen S, Ngai ECH (2020) Real-time air pollution monitoring with sensors on city bus. *Digital Commun Netw* 6(1):23–30
- Lee AJ, Diwekar UM (2012) Optimal sensor placement in integrated gasification combined cycle power systems. *Appl Energy* 99:255–264
- Ma Y, Richards M, Ghanem M, Guo Y, Hassard J (2008) Air pollution monitoring and mining based on sensor grid in London. *Sensors* 8(6):3601–3623
- Marjovi A, Arfire A, Martinoli A (2015) High resolution air pollution maps in urban environments using mobile sensor networks. In: 2015 International conference on distributed computing in sensor systems. IEEE, pp 11–20.
- Mihăiță AS, Dupont L, Chery O, Camargo M, Cai C (2019) Evaluating air quality by combining stationary, smart mobile pollution monitoring and data-driven modelling. *J Cleaner Production* 221:398–418
- Manfreda S, McCabe MF, Miller PE, Lucas R, Pajuelo Madrigal V, Mallinis G, Dor EB, Helman D, Estes L, Ciraolo G, Müllerová J, Tauro F, Isabel De Lima M, De Lima JLMP, Maltese A, Frances F, Caylor K, Kohv M, Perks M, Ruiz-Pérez G, Su Z, Vico G, Toth B, Müllerová J (2018) On the use of unmanned aerial systems for environmental monitoring. *Remote sensing* 10(4):641
- Milward R, Popescu GH, Michalikova KF, Musova Z, Machova V (2019) Sensing, smart, and sustainable technologies in Industry 4.0: Cyber-physical networks, machine data capturing systems, and digitized mass production. *Econ Manage Financial Markets* 14(3):37–43.
- Moltchanov S, Levy I, Etzion Y, Lerner U, Broday DM, Fishbain B (2015) On the feasibility of measuring urban air pollution by wireless distributed sensor networks. *Sci Total Environ* 502:537–547
- Mukherjee R, Diwekar UM (2016) Comparison of Monte Carlo and quasi-Monte Carlo technique in structure and relaxing dynamics of polymer in dilute solution. *Comput Chem Eng* 84:28–35
- Mukherjee R, Diwekar UM, Vaseashta A (2017) Optimal sensor placement with mitigation strategy for water network systems under uncertainty. *Comput Chem Eng* 103:91–102
- Mulholland JA, Butler AJ, Wilkinson JG, Russell AG, Tolbert PE (1998) Temporal and spatial distributions of ozone in Atlanta: regulatory and epidemiologic implications. *J Air Waste Manage Assoc* 48(5):418–426
- Nguyen LV, Hu G, Spanos CJ (2018) Efficient sensor deployments for spatio-temporal environmental monitoring. *IEEE Trans Syst Man Cybern Syst*
- Reis S, Seto E, Northcross A, Quinn NW, Convertino M, Jones RL, Maier HR, Schlink U, Steinle S, Vieno M, Wimberly MC (2015) Integrating modelling and smart sensors for environmental and human health. *Environ Model Softw* 74:238–246
- Richards M, Ghanem M, Osmond M, Guo Y, Hassard J (2006) Grid-based analysis of air pollution data. *Ecol Modell* 194(1–3):274–286
- Rico-Ramirez V, Reyes-Mendoza MA, Quintana-Hernandez PA, Ortiz-Cruz JA, Hernandez-Castro S, Diwekar UM (2010) Fisher information on the performance of dynamic systems. *Ind Eng Chem Res* 49(4):1812–1821
- Rockafellar RT, Wets RJB (1991) Scenarios and policy aggregation in optimization under uncertainty. *Math Oper Res* 16(1):119–147
- Ruszczynski A (1986) A regularized decomposition method for minimizing a sum of polyhedral functions. *Math Program* 35(3):309–333
- Sahin KH, Diwekar U, M. (2004) Better Optimization of Nonlinear Uncertain Systems (BONUS): a new algorithm for stochastic programming using reweighting through Kernel density estimation. *Ann Oper Res* 132:47–68
- Shastri Y, Diwekar UM (2006) Sensor placement in water networks: a stochastic programming approach. *J Water Resources Plan Manage* 132(3):192–203
- Sun C, Yu Y, Li VO, Lam JC (2019) Multi-type sensor placements in Gaussian spatial fields for environmental monitoring. *Sensors* 19(1):189
- TADA (2020) The Georgia Department of Transportation's Traffic Analysis and Data Application (TADA!) Maps © Thunderforest. Data © OpenStreetMap contributors. <https://gdottrafficdata.drakewell.com/publicmultinodemap.asp>. Accessed 12 May 2020
- Tmušić G, Manfreda S, Aasen H, James MR, Gonçalves G, Ben-Dor E, Anna B, Maria P, Jose Juan A, János M, Ruodan Z, Kasper J, Yoann M, Pedroso I, de Corine DL, Sorin H, Matthew M, Zhuang R (2020) Current practices in UAS-based environmental monitoring. *Remote Sensing* 12(6):1001
- Vochozka M, Rowland Z, Šuleř P (2019). The specifics of valuating a business with a limited lifespan. *Ad Alta: J Interdisciplinary Res* 9(2).

**Publisher's Note** Springer Nature remains neutral with regard to jurisdictional claims in published maps and institutional affiliations.

## Affiliations

Rajib Mukherjee<sup>1,2</sup> · Urmila M. Diwekar<sup>1</sup> · Naresh Kumar<sup>3</sup>

✉ Urmila M. Diwekar  
urmila@vri-custom.org

<sup>1</sup> Center for Uncertain Systems: Tools for Optimization & Management, Vishwamitra Research Institute, Crystal Lake, IL 60012, USA

<sup>2</sup> Department of Chemical Engineering, The University of Texas Permian Basin, Odessa, TX 79762, USA

<sup>3</sup> Electric Power Research Institute, Palo Alto, CA 94304, USA